# AN IN SITU SEM STUDY OF CRACK PROPAGATION

Michael Andersson[*], Christer Persson[*] and Solveig Melin[**]
[*] Division of Materials Engineering
[**] Division of Mechanics, Lund University, Sweden
Box 118, Lund University, Sweden
Michael.Andersson@material.lth.se

## Abstract

In this paper fatigue crack propagation in an aluminium alloy is studied using an in situ SEM technique. It is demonstrated that crack propagation is strongly dependent on the local conditions around the crack tip and that the nominal stress intensity factor is only an averaging parameter. It is also shown that the crack propagates mainly through a single slip mechanism and by joining of micro cracks.

## Introduction

It is well known that fatigue is caused by propagation of cracks under cyclic loading. Thus, the ability to understand fatigue and accurately calculate fatigue lives depends on the understanding of the mechanisms behind fatigue crack propagation. Also, detailed understanding of the various phenomena related to fatigue will improve the quality of life predictions and lead to better utilization of materials.

In this paper fatigue crack propagation in an aluminium alloy (AA2014) is studied by in situ scanning electron microscope (SEM) observations. The SEM has proven to be a very valuable tool for investigating fatigue growth mechanisms, see for instance Vehoff and Neumann [1], Andersson and Persson [2] or Zhang et al. [3]. This tool gives a unique possibility to follow the crack propagation cycle by cycle and to study the local conditions in the crack tip vicinity and thus to give new understanding to fatigue. Some phenomena, such as micro cracking ahead of the main crack or crack branching, are normally difficult to study. But with the use of the in situ SEM technique, it is possible to investigate these mechanisms.

The purpose of this work is to study the local interactions around the crack tip and to give better understanding of how they influence the crack propagation rate. The local deformation fields around the crack tip are measured directly from the SEM pictures in both mode I and mode II. From these measurements the crack tip opening and shear displacements (CTOD and CTSD) are calculated and compared to the crack propagation rate. Also, the influence from micro cracking and crack branching is discussed.

## Experimental work

The experiments were conducted on thin specimens of aluminium alloy AA2014 approximately 10 mm wide, with a total length of 70 mm and thickness varying between 0.5 mm and 0.8 mm, see Figure 1a. A sharp, V-shaped starter notch was created using a knife, and a crack was initiated by cyclic loading in a servo hydraulic tensile testing machine, resulting in a single edge crack. This crack geometry was chosen in order to have one well defined crack tip. Also, it is difficult to achieve a symmetrical crack growth for centre cracked specimens or specimens with double edge cracks. The use of a servo hydraulic machine for crack initiation was due to the limited load frequency possible in the SEM load stage. Crack initiation was performed at 20 Hz using the same load range ($\Delta\sigma = \sigma_{max} - \sigma_{min}$) and load ratio ($R = \sigma_{min}/\sigma_{max}$) as in the in situ experiments.
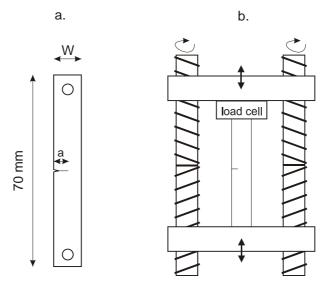
FIGURE 1. a. Test specimens and b the SEM load stage.

Crack initiation was stopped after some 10000 cycles when the crack length, *a*, had reached approximately 1-2 mm. Next, the specimens were transferred to the SEM load stage, placed inside the microscope. Here the load is applied by the turning of two screws using an electrical motor, thus moving the grips relative to each other, see Figure 1b. The force through the specimen is controlled by a load cell at one of the grips and the arrangement is controlled by a computer running LabView [4]. Before any measurements were performed, at least 100 cycles were allowed for the crack to stabilize after placement in the load stage. The load frequency in the in situ observations were approximately 0.1 Hz, slightly dependent on load levels. All SEM observations were performed at high vacuum, with a pressure less than $1.3 \cdot 10^{-4}$ mbar. Some specimens were removed from the SEM for further cycling in the servo hydraulic machine to allow for many load cycles to be run fast before continuing the measurements. Before the observations the specimens were ground with 500 grit paper and polished with 1 μm diamond paste. A summary of the experiments can be found in Table 1.

The measurements were made in intervals of between 10 and 100 cycles, taking an image at maximum load and then repeating the procedure. From the picture sequences the position of the crack tip can be followed, as seen in Figure 4a and b. Crack length was measured as the horizontal distance from the edge to the crack tip, i.e. the projected distance in the global mode I direction, parallel to the x-direction as shown in Figure 2. Thus, local deviations in crack propagation direction were not taken into account when measuring crack length and crack propagation rate. Crack propagation rate per cycle, *da/dN*, is calculated by dividing the measured crack extension by the number of cycles between two consecutive observations. It should be noted that crack extension by joining of micro cracks, see below, was not considered when measuring crack extension.

From the SEM-images it is also possible to study the mechanisms through which the crack propagates. Since it is believed that the local conditions in the crack tip vicinity have a decisive influence on the crack propagation it is interesting to get a local measure of the load exerted on the crack tip. To get such a local measure the displacements CTOD and CTSD are used. These parameters are calculated from the deformation between the crack surfaces, measured directly in the SEM-images.

TABLE 1. Summary of load cases.

| Load case | $\Delta\sigma=\sigma_{max}-\sigma_{min}$ (MPa) | $R=\sigma_{min}/\sigma_{max}$ | $a$ (mm) |
|---|---|---|---|
| 1 | 140 | 0.07 | 1.2-2.0 |
| 2 | 127 | 0.07 | 1.3 |
| 3 | 41.7 | 0.14 | 3.6 |
| 4 | 65.1 | 0.09 | 3.6 |
| 5 | 138 | 0.05 | 1.7 |
| 6 | 109 | 0.06 | 1.7 |
| 7 | 123 | 0.06 | 1.7 |

The deformation is defined as half the distance, as the crack is loaded with maximum load in the cycle, between two points that are in contact when the crack is closed. The opening deformation is measured in the global $y$-direction and shear deformation in the $x$-direction. The measurements are taken in discrete points as a function of the distance $x$ from the crack tip. For the opening displacement, $u_y$, 8-10 measuring points were taken at uniformly spaced intervals for a distance some tens of micrometers from the crack tip. For the shear deformation, $u_x$, it is necessary to chose points that can be identified as contacting points for the closed crack, typically corners where the crack path changes direction. This requirement limits the number of measuring points somewhat for the shear displacements.

To reduce the measured points into separate single parameters for opening and shear deformation it is assumed that the crack has a shape of the form:

$$u_i = A_i x^{b_i}, \qquad i = x, y \qquad (1)$$

where $u_i$ are the displacements in the $x$ and $y$ directions, $x$ the distance from the crack tip and $A_i$ and $b_i$ are constants. This expression was fount to fit the experimental data well, also it is in analogy with analytical solutions to crack problems. Next the intersections with the fitted expressions and the $\pm45°$ lines, as seen in Figure 3 where found and the crack tip displacements defined as $2u_i$ at these points.
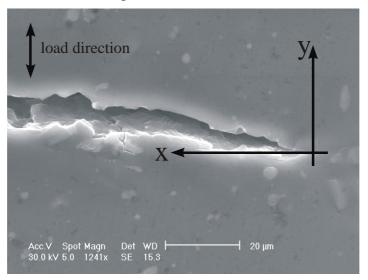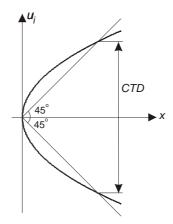


FIGURE 2. Coordinate directions around the crack tip.

FIGURE 3. The definition of crack tip opening and shear displacement.

## Results and discussion

The in situ SEM technique for fatigue crack propagation experiments provides unique possibilities to study phenomena and mechanisms related to fatigue. The technique is however not without limitations. Obviously the observations are restricted to the surfaces and processes in the centre of the specimens cannot be directly studied. The use of thin specimens somewhat reduces this limitation since the surface is representative for the entire cross section. Though, fractographic examinations sometimes reveal differences over the thickness even for specimens as thin as 0.5 mm.

The other limitation concerns load magnitude and frequency. The load stage used in these tests has a maximum load of approximately 5 kN and maximum load frequency of around 0.2 Hz. The low load frequency makes it necessary to use a servo hydraulic machine for crack initiation.

Finally, the SEM operates at low pressures, close to vacuum. Some microscopes, such as the one used in this study, have been fitted with an environmental chamber that makes it possible to run testing in a gaseous or moist environment, though still at low pressures. Thus, even if it is possible to have for instance an oxidizing environment it is not possible to simulate real operating conditions for most applications.

### *Crack propagation rate*

From traditional fatigue crack propagation experiments it is expected that there is a strong correlation between crack propagation rate per cycle, *da/dN*, and applied stress intensity range, $\Delta K = K_{max} - K_{min}$. In Figure 5 *da/dN* is plotted against $\Delta K$, calculated from handbook solutions, found in for instance Tada et al. [5], and measured crack length and applied load. From the figure it is obvious that there is no correlation between *da/dN* and $\Delta K$, a fact that is contradictory to many experimental studies, cf. for instance Paris et al. [6] or Hahn and Simon [7]. This difference is believed to stem from the way the crack propagation rate is measured. In this study *da/dN* is measured over rather few cycles and short distances, where local factors, such as deviations in crack path, become very influential. If *da/dN* was measured over more cycles and longer distances the local effects average out and $\Delta K$ is a useful parameter. It should also be noted that the variations in specimen thickness could have some influence on the results. This is, however, not sufficient to explain the total scatter in the results.

To further investigate the importance of the local effects the relation between nominal $\Delta K$ and CTOD, measured from the crack profiles, was studied. Based on the elastic solution

found in for instance Anderson [8], it is expected that CTOD in the plane stress case is calculated from $K_I$ as:

$$CTOD = \frac{16}{\pi}\left(\frac{K_I}{E}\right)^2 \qquad (2)$$

with $K_I$ denoting the global mode I stress intensity factor and $E$ denoting Young's modulus. In Figure 6 the result is shown, with the solid line corresponding to equation (2). It is obvious that there is a high degree of scatter and little correlation. It is also seen that for most data points the measured crack tip opening displacement is higher than the calculated one. This is a result of local plastic deformation and to some extent crack path deflections.

Furthermore, it is interesting to see if *da/dN* can be correlated to measured CTOD. In Figure 7a the experimental data are shown, and solid line shows mean propagation rate at a given CTOD. In the figure it is seen that there is a correlation between *da/dN* and CTOD, even if the scatter is higher than expected. But since there is a mode II component in the local deformation field the crack tip displacement, CTD, is introduced as:

$$CTD = \sqrt{CTOD^2 + \alpha \cdot CTSD^2} \qquad (3)$$

with $\alpha$ being a constant fitted from the experimental data to minimize the scatter in the CTD-*da/dN* relation. In Figure 7b the result is shown. The scatter is somewhat lowered, especially for some points where CTOD is low but there is a strong CTSD component. This further shows that the local displacements, CTOD and CTSD, interact strongly. However, there is still a high degree of scatter in the data.

There are two main reasons for the scatter. First it can be discussed how *da/dN* is measured. As mentioned earlier, by taking the projected crack extension deflections, the actual crack path is not included in *da*. A more accurate method would be to take the total
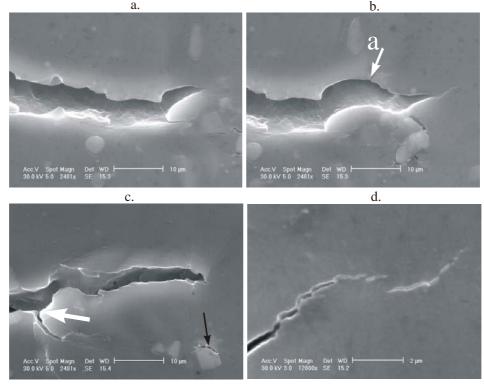


FIGURE 4. a. and b. Crack propagation over 10 cycles. c. Crack branching (white arrow) and micro cracking (black arrow). d. Crack growth by joining of micro cracks.

integrated increase in crack length, including local deflections. This approach could, on the other hand, introduce subjectivity since there is a limit for how small deflections that can be measured. The other reason for the scatter is the way CTOD and CTSD are determined. Here the global directions are also used, not accounting for deflections and questions might be raised on the assumed crack shape in equation (1).

There are other ways to calculate the crack tip displacements. One alternative way of defining the crack tip opening displacement would be to take the opening at a given distance from the tip, as in for instance Blochwitz et al. [9]. However, since both opening and shear displacements are of interest, this approach is not applicable here, also it could be debated how the distance should be chosen. Other crack shapes could also be assumed, as in for instance [9].

For a future study it might be of interest to measure crack extension along one direction, before any deflections, and to take crack opening perpendicular to the propagation direction.

### *Crack propagation mechanisms*

The in situ SEM technique is also a powerful tool to study the mechanisms involved in fatigue crack propagation. Usually it is assumed that in stage II, as in the present study, crack propagation occurs through a double slip mechanism, as suggested by Laird [10] or Pelloux [11]. There are also some experimental data suggesting this mechanism, cf. [1] or Neumann et al. [12]. However, in these experiments is seen that a single slip band eminates from the crack tip and crack growth occurs by a singe slip decohesion mechanism, see Figure 4b. This behaviour has been noted by other also, see Zhang [13], [1] or [2]. In this study it was also seen that if two slip bands were simultaneously created at the crack tip, branching occurred, as in Figure 4c. After branching one of the cracks eventually stopped while the other continued as the main crack. In some cases the two branches joined up again to a single crack.

Another important crack propagation mechanism is growth by joining of micro cracks. Creation of small cracks was often observed ahead of the main crack, as seen in Figure 4d. These micro cracks contributed to crack propagation by growing and after some cycles joining with the main crack. Cracks were also created at the interface between the bulk material and intermetallic precipitates, see Figure 4c. This behaviour is a result of the stress concentrations induced by the particles and the mismatch in elastic properties between the intermetallic and the aluminium.
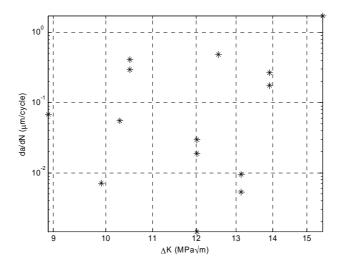


FIGURE 5. Crack propagation rate as a function of the nominal stress intensity factor.
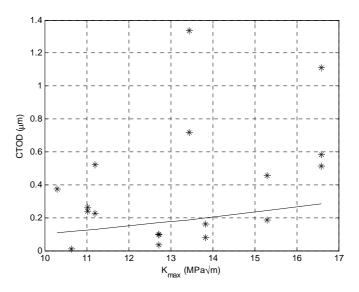
FIGURE 6. Relationship between applied stress intensity factor and crack tip opening displacement.

Finally it should be noted that crack closure was observed for all load cases, i.e. the crack surfaces were in contact for a part of the load cycle, even though a tensile load was applied at all times. This is a well known phenomenon, described by for instance Elber [14,15] or see Suresh [16] where a general discussion on the phenomena can be found. In this study two types of crack closure was noticed. Firstly, plasticity induces closure, caused by the plastic crack wake, was seen. Secondly, roughness induced closure was observed, resulting from the crack path deflections. This mechanism was found to have a strong influence on the crack propagation, and points on the crack surfaces were at times seen to have contact even at maximum load. These phenomena further stress the importance of local effects.
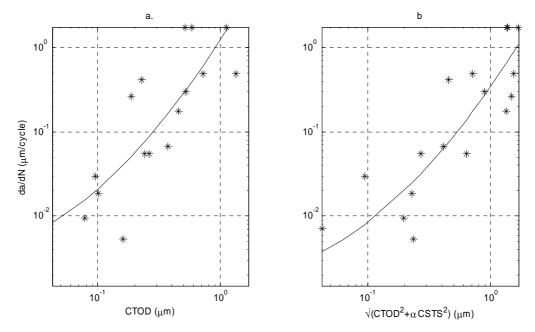


FIGURE 7. Crack propagation rate as a function of a. crack tip opening displacement and b. combination between crack tip opening and shear displacement.

## Conclusions

It has been shown that crack propagation is a very local phenomenon that is strongly influenced by the conditions in the vicinity of the crack tip. A nominal stress intensity range may work well in an averaging situation but is not useful to describe processes close to the crack tip. Furthermore it was seen that the crack propagation rate is influenced by local mode I as well as mode II displacements. The mixed mode is a result of local deflections in the crack path.

Crack growth was found to occur mainly by a single slip decohesion mechanism along a single slip band. Two simultaneous slip bands promoted branching. Also contributing to the crack growth, micro cracking ahead of the crack tip and at intermetallic particles was frequently seen.

## Acknowledgement

## References

1. Vehoff, H. and Neumann P., *Acta Metall.*, vol. **27**, 915-920, 1979

2. Andersson H. and Persson C., *Int. J. Fatigue*, vol. **26**, 211-219, 2004

3. Zhang X.P., Wang C.H., Ye, L. and Mai, Y.W., *Fatigue Fract. Eng. Mater. Struct.*, vol. **25**, 141-150, 2002

4. National Instruments Corporation, *LabVIEW User Manual*, National Instruments, 1998

5. Tada H., Paris P.C. and Irwin G.R., *The Stress Analysis of Cracks Handbook*, Third edition, ASME Press, New York, U.S., 2000

6. Paris, P.C., Gomex, M.P. and Anderson W.E., *The trend in engineering*, vol. **13**, 9-14, 1961

7. Hahn C.T. and Simon R., *Eng. Fract. Mech.*, vol. **5**, 523-540, 1973

8. Anderson, T.L., *Fracture Mechanics*, Second edition, CRC Press, 1995

9. Blochwitz C., Tirschler W. and Weidner A., *Mater. Sci. Eng.*, A357, 264-269, 2003

10. Laird C., *Fatige Crack Propagation, ASTM STP 415*, American Society for Testing and Materials,131-168, 1967

11. Pelloux R.M.N., *Eng. Fract. Mech.*, **vol**. 1, 697-704, 1970

12. Neumann, P., Vehoff H. and Fuhlrott H., In *Proceedings of the Fourth International Conference on Fracture*, vol. **2**, 1313-1324, 1977

13. Zhang. J.Z., *Eng. Fract Mech.*, vol **65**, 665-681, 2000

14. Elber, W., *Eng. Fract Mech.*, vol **2**, 37-45, 1970

15. Elber W., *Damage Tolerance in Aircraft Structures, ASTM STP 486*, American Society for Testing and Materials, 230-242, 1971

16. Suresh, S., *Fatigue of Materials*, Second edition, Cambridge Univeristy Press, Cambridge, U.K., 1998